APPLIED MATERIALS AND TECHNOLOGY

Jamt.ejournal.unri.ac.id

Research Article

Antimicrobial properties of silver/graphene oxide nanocomposite prepared by redox chemical reaction

Maria Elena Leyva González[1,*], Rosana Ribeiro Rodrigues[1], Igor Luiz dos Santos[1], Adhimar Flávio Oliveira[1], Estácio Tavares Wanderley Neto[2], Fabio Nakagomi[1], Paulo Sergio Marques[3], Eder do Couto Tavares[1]

ABSTRACT: Silver nanoparticles (AgNPs) exhibit outstanding antimicrobial properties, making them highly valuable in biomedical applications. This study presents the synthesis of a graphene oxide-silver nanoparticle (GO-Ag) nanocomposite via a redox chemical reaction, where the hydroxyl groups reduced silver ions present in graphene oxide (GO). Graphene oxide was obtained through electrochemical exfoliation of graphite, followed by ultrasonic exfoliation in the presence of silver ions to form GO-Ag. The materials were characterized using ultraviolet-visible (UV-Vis) spectroscopy, Fourier transform infrared (FTIR) spectroscopy, Raman spectroscopy, scanning electron microscopy (SEM), and X-ray diffraction (XRD). UV-Vis, FTIR, and Raman spectra confirmed GO synthesis. In contrast, XRD and UV-Vis spectra verified the presence of silver nanoparticles in GO-Ag by detecting the surface plasmon resonance (SPR) band and silver's characteristic diffraction peaks. SEM analysis showed the successful formation of silver nanoparticles on GO sheets. The disc diffusion method assessed Antimicrobial activity against Staphylococcus aureus (Gram-positive) and Escherichia coli (Gram-negative). GO-Ag nanocomposite displayed significant antibacterial activity, as evidenced by the formation of inhibition zones, whereas GO alone showed no antimicrobial effect. The enhanced antibacterial properties of GO-Ag are attributed to the synergistic interaction between GO and AgNPs. The increased surface area of silver nanoparticles further enhances their antibacterial effectiveness by facilitating better interaction with bacterial membranes. These findings highlight GO-Ag's potential for use in antimicrobial coatings, wound dressings, and biomedical devices. This study demonstrates an effective, environmentally friendly approach to synthesizing antimicrobial nanocomposites, paving the way for their application in various medical and industrial fields.

Keywords: *Silver nanoparticles, graphene oxide, antimicrobial, nanosheets*

1. INTRODUCTION

Silver nanoparticles (AgNPs) are considered essential active ingredients in various biomedical applications [1]. Due to their unique antibacterial properties, they are widely used as sterilizing agents in dental and surgical procedures, wound and burn treatments, and biomedical devices [2]. Additionally, AgNPs have antimicrobial applications in other fields, including surface cleaning, textiles, food storage bags, and air purification systems [2-4]. The antimicrobial action of AgNPs is well known, firstly, due to their large surface areas they can connect to bacterial biomolecules. Then AgNPs act as a delivery system for free silver ions. Due to their positive charge, silver ions are electrostatically attracted to sulfur-containing proteins, allowing them to adhere to bacterial cell walls and cytoplasmic membranes. Once attached, silver ions compromise membrane integrity and permeability, ultimately leading to cell membrane disruption [5].

Nanomaterials are defined as materials with dimensions ranging from 1 to 100 nm, which results in a larger surface area [6]. Nanoparticles are formed by the assembly of atoms or molecules of a given material. Regardless of whether the

OPEN ACCESS

Affiliation

[1]Federal University of Itajubá, Physical Chemistry Institute

[2]Federal University of Itajubá, Institute of Electrical Systems and Energy. High Voltage Laboratory

[3]Federal University of Itajubá, Institute of Natural Resources. Microbiology Laboratory

***Correspondence**

Email: mariae@unifei.edu.br

ORCID

Maria Elena Leyva González: 0000-0003-0673-5713
Rosana Ribeiro Rodrigues: 0009-0009-5005-3905
Igor Luiz dos Santos: 0009-0006-2601-1287
Adhimar Flávio Oliveira: 0000-0003-2586-7359
Estácio Tavares Wanderley Neto: 0000-0002-1241-7378
Fabio Nakagomi: 0000-0001-6538-2239
Paulo Sergio Marques: 0000-0003-0330-0933
Eder do Couto Tavares: 0000-0001-5228-4912

Received: January 27, 2025
Revised: February 22, 2025
Accepted: February 26, 2025

How to cite: Ribeiro Rodrigues, R., Luiz dos Santos, I., Elena Leyva González, M., Nakagomi, F., Tavares Wanderley Neto, E., Sergio Marques, P., Flávio Oliveira, A., & do Couto Tavares, E.. (2025). Antimicrobial properties of silver/graphene oxide nanocomposite prepared by redox chemical reaction. Journal of Applied Materials and Technology, 6(1), 21–29. https://doi.org/10.31258/Jamt.6.1.21-29.

synthesis method follows a top-down or bottom-up approach, a stabilizing agent is required to control nanoparticle size and prevent aggregation. Among bottom-up approaches, chemical reduction is the most commonly used method [6]. Notably, certain reduction techniques utilize a reducing agent that simultaneously acts as a capping material, which is particularly advantageous.

Graphene oxide (GO) is an intermediate material in the chemical or electrochemical production of graphene [7]. It consists of nanosheets functionalized with oxygen-containing groups (epoxy, carboxyl, and hydroxyl), which stack together to form layered structures ranging from the nanoscale to the microscale [8]. Due to these properties, GO nanosheets serve as potential precursors for nanosilver particles, acting as capping materials, while oxygen functional groups can act as reducing agents for silver ions.

There are several works that show the antibacterial properties of graphene oxide and silver nanoparticles nanocomposite. However nearly all nanocomposites are obtained using different reducing agents [9]. Few works show the graphene oxide as a potential reducing agent of metallic ions [10]. Therefore, our main objective is to show that it is possible the synthesis of graphene oxide -silver nanoparticle (GO-Ag) by a simple redox chemical reaction. We checked the obtaining of GO-Ag nanocomposite by several techniques of characterization and evaluated its antimicrobial activity.

2. MATERIALS AND METHODS

A current source (Model FA-3005 Digital 1-channel, Instrutherm) with a voltage capacity of up to 32 V and a current limit of 5 A was used for the electrochemical exfoliation process. An electrolytic cell was assembled using commercial graphite electrodes as the working electrode (anode) and counter electrode (cathode), with a 0.1 M sulfuric acid (H_2SO_4) solution serving as the electrolyte (Figure 1).

The exfoliation process began with applying a direct current (DC) voltage of +2.3 V for 5 minutes. The voltage was subsequently increased in increments of +3 V every 5 minutes until reaching +13 V, maintaining each step for 5 minutes. After exfoliation, the resulting graphene oxide (GO) was filtered and thoroughly washed with distilled water using gravity filtration until a neutral pH was achieved. The GO product was then dried in an oven at 60°C for 24 hours.

The obtained GO was dispersed in distilled water at a concentration of 0.1% by mass (0.01 g in 10 mL of distilled water). To further exfoliate the GO and enable the chemical reduction of silver ions, an ultrasonic bath (42 kHz) was applied in the presence of a 1 mM aqueous silver nitrate ($AgNO_3$) solution. The ultrasonication process was conducted for 60 minutes per day over 5 consecutive days, totaling 5 hours. After ultrasonication, the GO-$AgNO_3$ dispersion was filtered and thoroughly washed with distilled water using gravity filtration. The final product was dried in an oven at 60°C for 24 hours. The scheme presented in Figure 1 illustrates the entire sequence.

For UV-Vis characterization, a 1 mL aliquot of the GO-Ag dispersion (before filtration) was diluted in 2 mL of distilled water. Absorbance measurements were conducted using a Karvi K37-UVVIS spectrophotometer, operating in the wavelength range of 190 to 1100 nm.

The chemical structure of the samples was analyzed using Fourier-transform infrared (FTIR) spectroscopy in transmission mode. The samples were prepared in KBr pellets, and the spectra were recorded in the wavenumber range of 650 to 4000 cm^{-1} at room temperature. The analysis was performed using a Shimadzu IRTracer-100 spectrometer, with an average of 32 scans per spectrum and a resolution of 8 cm^{-1}.

The microstructure of the GO-Ag powder was characterized by X-ray diffraction (XRD). The diffraction patterns were collected using a Malvern Panalytical X'Pert PRO diffractometer equipped with CuKα radiation (λ = 1.5406 Å) and a graphite monochromator. The scanning range (2θ) was set between 5° and 50° with intervals of 0.02° and a scanning speed of 5.0 s per step. Raman spectroscopy was performed at room temperature using a Labram HR Evolution spectrometer with a green laser (λ = 532 nm) as the excitation source.

The morphology of the GO-Ag powder samples was examined using scanning electron microscopy (SEM). A Zeiss EVO MA 15 SEM was used, operating with an acceleration voltage of 15 kV and a working distance (WD) of 16-19 mm. The samples were fixed on double-sided carbon tape and were not gold-coated before analysis.

The antimicrobial efficacy of GO-Ag was evaluated using the disc diffusion method for antimicrobial susceptibility testing. Sterile filter paper discs were impregnated with 10 µL of the studied GO-Ag dispersion and placed on Mueller-Hinton agar plates previously inoculated with bacterial cultures.

The bacterial strains tested were Staphylococcus aureus (Gram-positive) and Escherichia coli (Gram-negative). These strains were collected from preserved culture plates and suspended in a sterile saline solution (0.9% NaCl). The bacterial suspensions were standardized to a concentration of 10^8 CFU/mL using the McFarland 0.5 scale and evenly spread on the agar plates using sterile swabs. The prepared paper discs were placed on the agar surface, and 10 µL of the antimicrobial solutions were applied. The plates were incubated at 37°C for 24 hours. After incubation, the inhibition zones (areas of bacterial growth inhibition around the discs) were measured in millimeters. Larger inhibition zone diameters indicated higher antimicrobial activity. All tests were performed in triplicate to ensure statistical reliability.

The methodology employed enabled the detailed synthesis and characterization of GO-Ag, ensuring the quality of the produced material. The combination of electrochemical exfoliation and ultrasonication proved to be effective in obtaining functionalized graphene oxide. The applied analytical techniques provided relevant structural and morphological information, while the antimicrobial tests demonstrated the material's biological activity, indicating its potential for applications in biomedical and technological fields.

3. RESULTS AND DISCUSSION

The large literature on graphene oxide shows that the oxygen functional groups are located both in the basal region and at the edges of the graphene nanolayers. In the basal region GO contains mainly epoxides and hydroxyl groups and at the edges can be found a low concentration of carbonyls, catechol, quinones, carboxylic acids, phenols and lactones [11]. Hydroxyl groups in basal regions are tertiary alcohol, therefore non-oxidizable. The catechol group

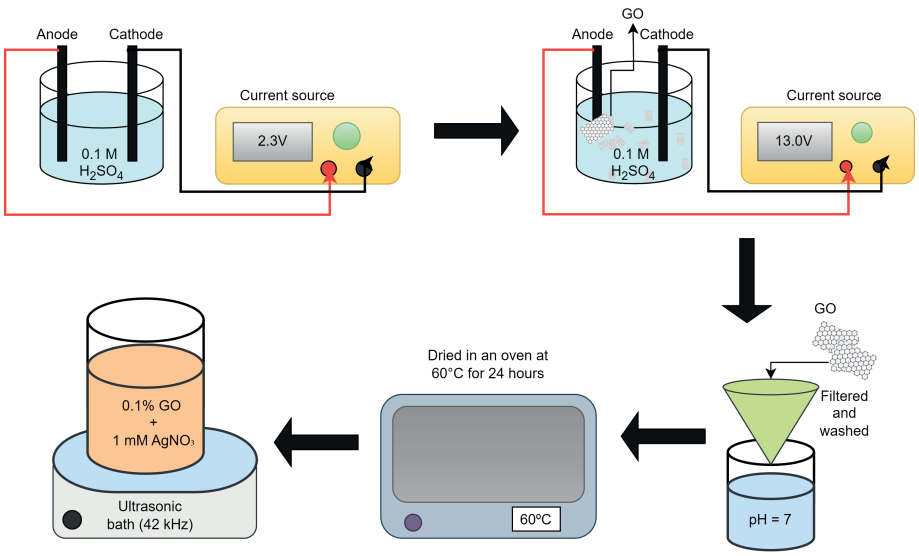

Figure 1. GO-Ag preparation scheme.

at the edges can be oxidized to quinone reducing ionic silver [12]. The redox chemistry reaction can be described as shown the Equation 1. Next, we discuss the physical-chemical characterization of the GO and graphene oxide-silver nanoparticle (GO-Ag) samples, to show that redox chemistry reaction occurred during to exfoliation of GO sheets in the presence of ionic silver, at an ultrasonic bath.

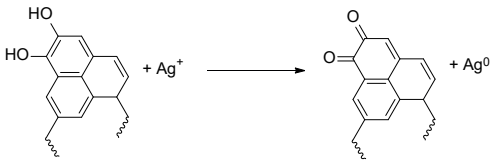

(1)

Figure 2 shows the UV-Vis spectrum of the aqueous dispersion of GO and GO-Ag. In the GO spectrum, a low-intensity band is observed at 226 nm. This electronic transition band is attributed to the π-π* transition of the C=C bonds in the aromatic rings that make up the GO layers [13]. The increase in the baseline in the wavelength region below 300 nm suggests visible light absorption, which can be attributed to functional groups. The lower-energy n-π electronic transition observed around 266 nm may result from the presence of functional groups such as -OH, C=O, and COOH.

UV-vis spectrum of GO-Ag shows a broad absorption band near 292 nm attributed to the n-π electronic transition band of GO. The band near 360 nm corresponds to the surface plasmon resonance (SPR) of silver nanoparticles [14]. Therefore, it is concluded that the hydroxyl and epoxy groups present on the surface of GO may reduce ionic silver (Ag^+) to metallic silver (Ag^0). Additionally, the band observed at 205 nm can be attributed to ionic silver (Ag^+) [15].

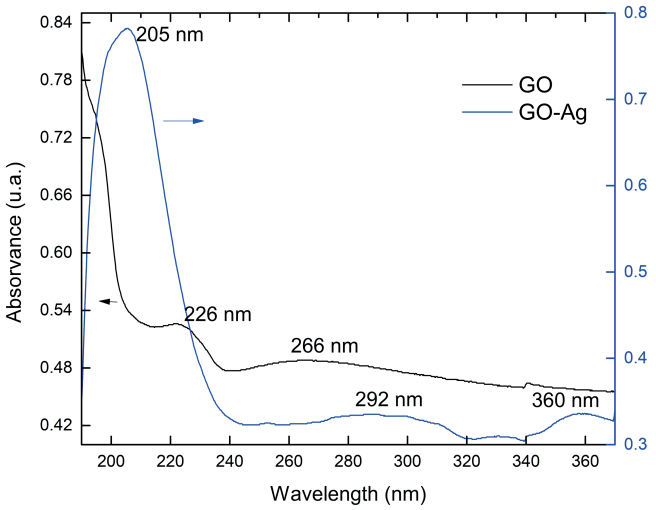

Figure 2. UV-vis spectrum of aqueous dispersion of GO and GOAg.

Figure 3 shows the FTIR spectrum of (a) GO and (b) GO-Ag powder. The characteristic vibrational bands observed in the FTIR spectrum of GO are as follows: an absorption band at 1053 cm^{-1}, corresponding to the stretching vibration of the C-O bond; a band at 1394 cm^{-1}, corresponding to the bending vibration of C-OH bond of carboxylic acid (COOH); an absorption band at 1569 cm^{-1}, corresponding to the stretching vibration of the C=C bonds in the aromatic rings; a lower intensity band at 1729 cm^{-1} corresponding to the stretching vibration of the C=O bond and a broad band at 3450 cm^{-1}, corresponding to the stretching vibration of O-H [16, 17]. The spectrum confirms the oxidation of graphite during the electrochemical exfoliation process, resulting in graphene oxide.

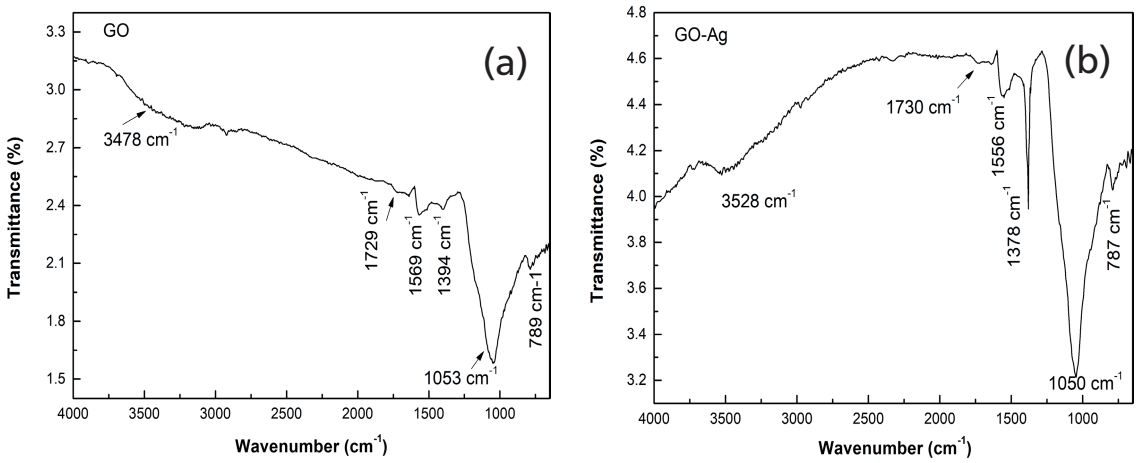

Figure 3. FTIR Spectrum of (a) GO and (b) GO-Ag.

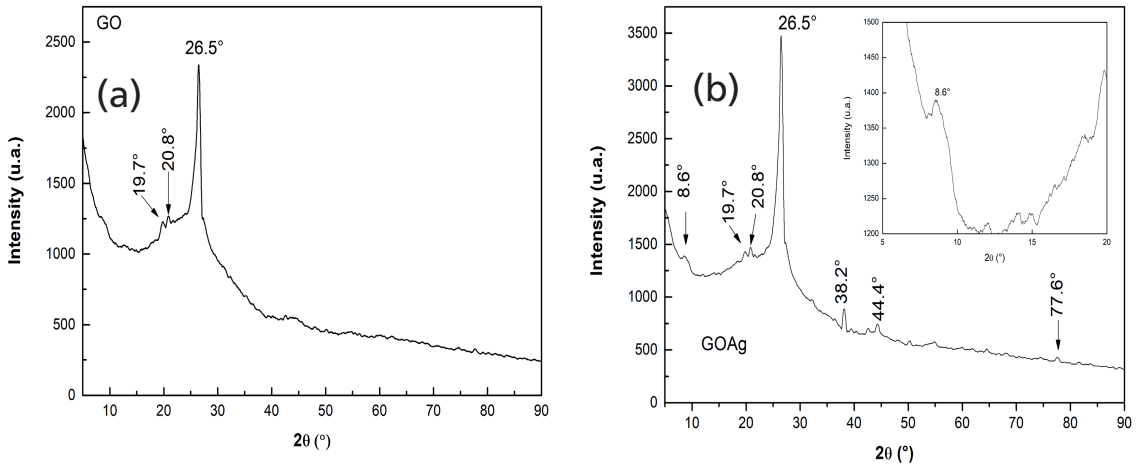

Figure 4. XRD Spectrum of (a) GO and (b) GO-Ag.

FTIR spectrum of GO-Ag shows vibration bands observed in GO. The ratio between the area of absorption bands at 1394 cm^{-1} and 1569 cm^{-1} assigned to vibration of bond C-OH and C=C of GO is the same 0.7. The ratio between the area of 1378 cm^{-1} and 1556 cm^{-1} bands to GO-Ag is 2.95. The results show a higher concentration of carboxylic acid groups at GO-Ag. This suggests that quinone groups are oxidized to carboxylic acid during the reduction of ionic silver. A displacement to a less wavenumber of C-O and C=C absorption bands suggest a lower strength of these chemical bonds. This decrease in strength bond can be due to the presence of Ag nanoparticles.

Figure 4(a) displays the XRD spectrum of GO. The diffraction peak at 2θ = 26.5° is characteristic of graphite, confirming the presence of this crystalline structure. The peaks around 2θ = 19.7° and 20.8° are also attributed to the crystalline structure of expanded graphite oxide [18].

In the XRD spectrum shown in Figure 4(b), a low-intensity peak at 2θ = 8.6° corresponds to GO [19]. This diffraction peak does not appear in the GO spectrum, suggesting that in this system, the graphene oxide sheets remain stacked after electrochemical and ultrasonic exfoliation, forming a graphitic structure. However, after ultrasonic exfoliation in the system containing silver, the graphene oxide sheets are stabilized.

Figure 4(b) also shows the characteristic diffraction peaks of metallic silver, confirming the reduction of Ag^{+} ions. In the GO-Ag system, peaks are observed at 2θ values of 38.2° (111), 44.4° (200) and 77.6° (311) [20]. These results are significant, as they confirm the differences in the crystalline structure of metallic silver reduced by GO. The average crystallite size of Ag^{0} was calculated using the Scherrer equation based on the diffraction peak at 2θ = 38.2° [21].

$$D = \frac{k\lambda}{\beta cos\theta}$$

Where D is the average crystallite size, k is the Scherrer constant, and λ is the wavelength of the incident X-ray (for Cu Kα, λ = 0.154056 nm), while β and θ represent the full width at half maxi-

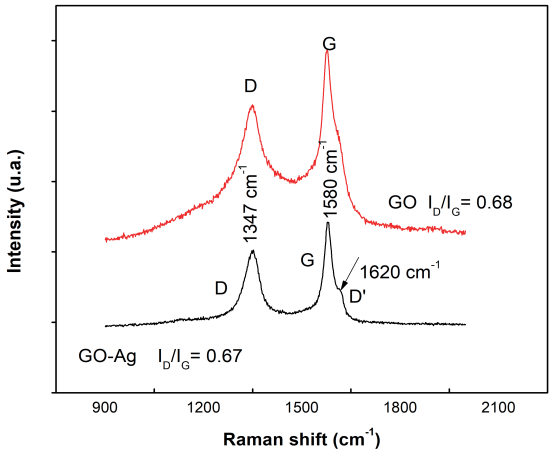

Figure 5. Raman Spectrum of (a) GO and (b) GO-Ag.

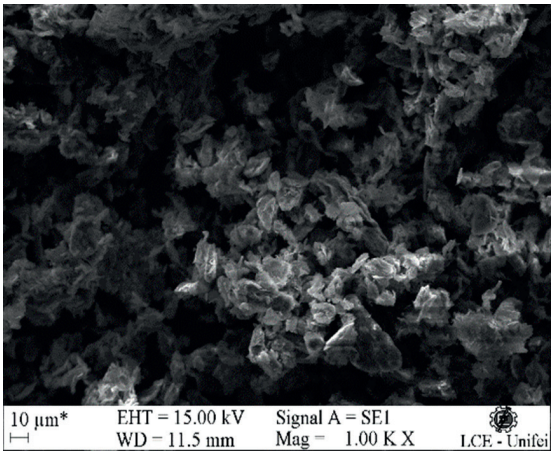

Figure 6. SEM Micrograph of GO.

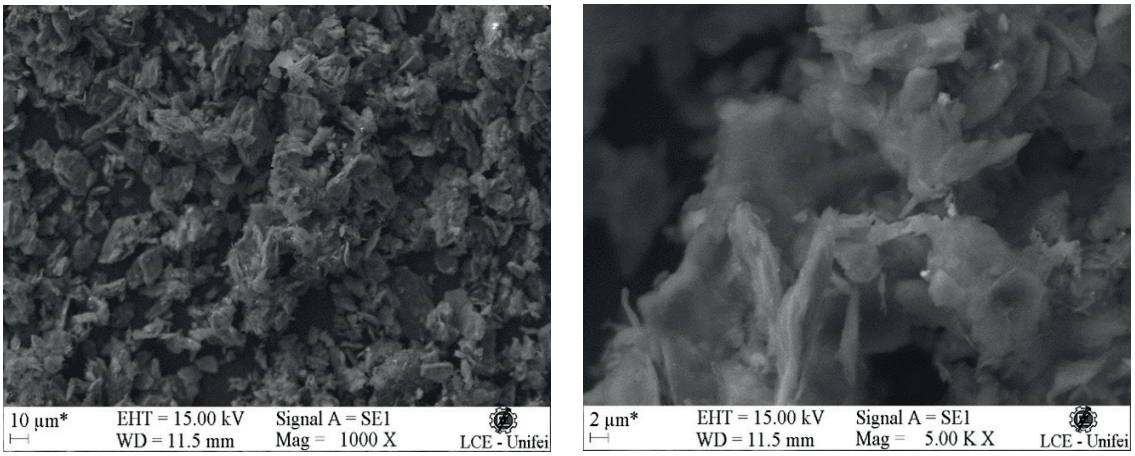

Figure 7. SEM Micrograph of GO-Ag. The image on the right shows an amplification of 1.00KX, while the image on the left shows an amplification of 5.00KX.

mum of the intensity and the Bragg angle, respectively. The crystallite size of metallic Ag reduced by GO, calculated using the Scherrer equation, was 15.5 nm. This average crystallite size is consistent with the SPR absorption band observed in the UV-Vis spectrum.

Figure 5 shows a comparative analysis of the Raman spectra for GO and GO-Ag. The Raman spectrum of both samples displays typical peaks at 1347 and 1580 cm^{-1}, corresponding to the D and G bands, respectively. The shoulder at 1620 cm^{-1} observed in Raman spectra of GO-Ag, known as the D' band, shows a phonon confinement caused by defects. The degree of disorder in the carbon structure is characterized by the intensity ratio between the D and G bands [22]. The I_D/I_G ratio of 0.68 for GO suggests a lower amount of disorder and defects and, therefore, a lower level of oxidation.

The I_D/I_G ratio of the GO-Ag material shows the same value as observed in GO. This result suggests that there is no change in the disordered structure of GO. In other words, the sp^3-hybridized carbon atoms, resulting from chemical functionalization, remain intact. Therefore, the Ag^o ions are reduced to Ag^o by the catechol hydroxyl groups when they are oxidized to quinone. Also, the D´ band observed in the Raman spectrum of OG-Ag suggests that the OG sheets act as capping of silver nanoparticles.

Figures 6 and 7 display the SEM micrographs of the GO and GO-Ag materials, respectively. The observed morphology supports the XRD results: the exfoliation of graphite does not result in a stable system, with GO sheets aggregating and forming complex and diverse morphologies [23]. The SEM-EDS images in Figure 8, related to the GO-Ag sample, confirm the presence of well-distributed silver nanoparticles (AgNPs) in the sample.

The microbiological characterization is presented below in Figures 9 and 10. Figure 11 summarizes the results from the column graph of the inhibition zone for the studied systems. The results show that the GO does not exhibit antimicrobial activity. We believe that this is due to the graphitic structure of the system, as confirmed by the XRD spectrum and morphology. However, the systems containing silver nanoparticles (AgNPs) demonstrated antimicrobial activity against both tested bacterial strains.

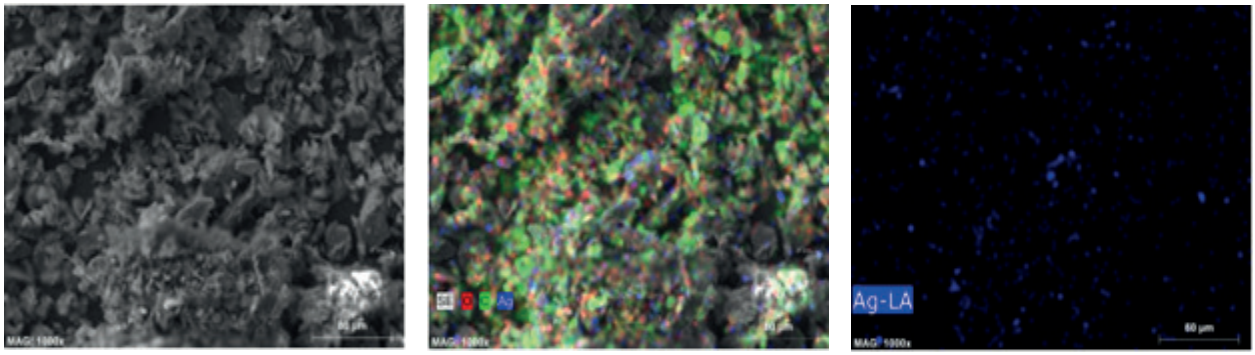

Figure 8. SEM-EDS Micrograph of GO-Ag.

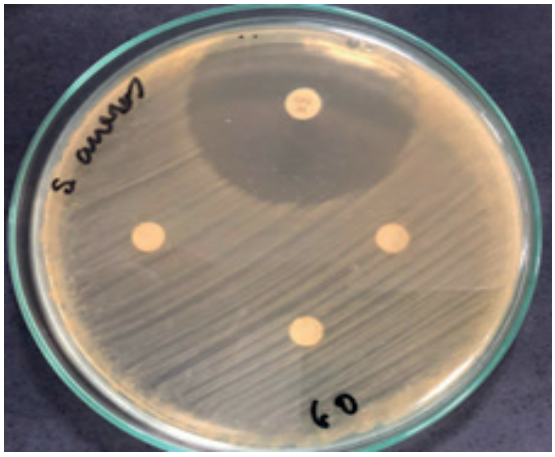

Figure 9. Antibiogram of the GO system.

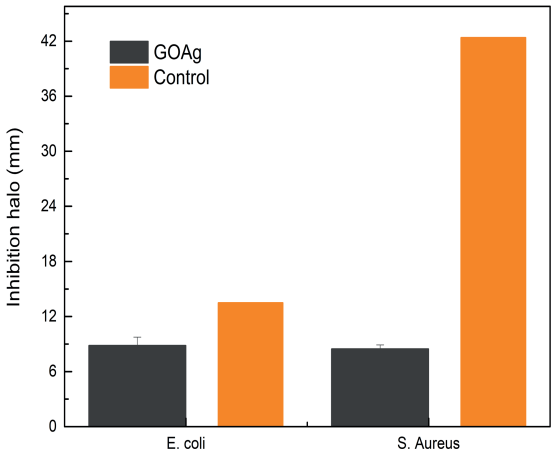

Figure 11. Inhibition halo of the studied systems and the positive control.

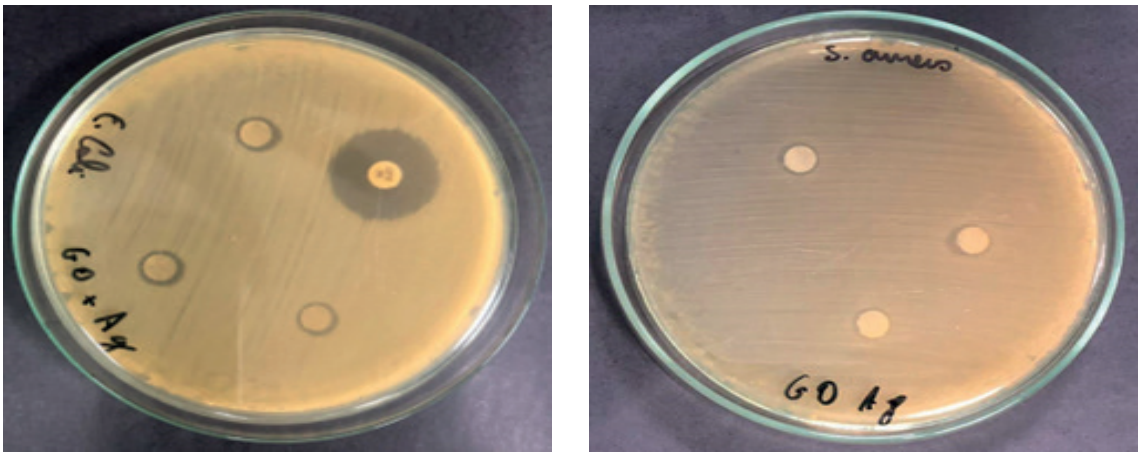

Figure 10. Antibiogram of the GO-Ag system.

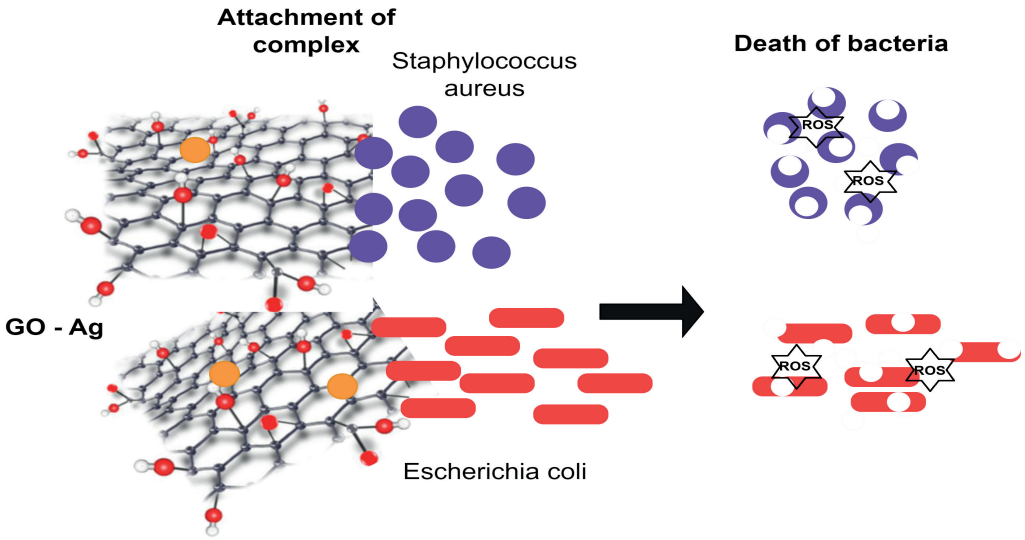

Figure 12. Symbolic representation of the antibacterial mechanism of the GO-Ag nanocomposite. The illustration shows the interaction of the nanocomposite with bacterial cells, leading to reactive oxygen species production, membrane disruption, and bacterial cell death. In the Figure, orange spheres represent AgNPs, red spheres represent oxygen atoms, black spheres represent carbon atoms, and white spheres represent hydrogen. The reactive oxygen species (ROS) that can cause bacterial cell death.

Figure 11 shows the inhibition zones, with both systems exhibiting antimicrobial activity against the two tested bacterial strains. The GO-Ag nanocomposite is more efficient, suggesting that the silver reduced from GO exhibits greater antimicrobial activity.

This shows that while GO alone does not exhibit antimicrobial activity, the incorporation of AgNPs significantly enhances the antimicrobial properties of the GO-Ag nanocomposite [24]. XRD and SEM analyses confirmed that the reduction of silver ions to metallic silver by GO does not alter the basic graphitic structure of GO but introduces effective antimicrobial agents. The increased inhibition zones observed for the GO-Ag system, compared to GO alone, highlight the superior antimicrobial activity provided by the silver nanoparticles. This suggests that the GO-Ag nanocomposite holds potential for applications requiring antimicrobial functionality, leveraging the synergistic effects of silver nanoparticles and graphene oxide. The GO sheets act as a supporting and stabilizing agent of silver nanoparticles. Therefore, GO increases the antimicrobial properties of silver nanoparticles acting in two ways: maximizing the contact area between AgNPs and the bacteria and avoiding the agglomeration of silver nanoparticles [25].

To further illustrate the antibacterial mechanism of the GO-Ag nanocomposite, Figure 12 presents a symbolic representation of the interaction between the nanocomposite and bacterial cells, highlighting the role of silver nanoparticles in enhancing antimicrobial activity [26].

4. CONCLUSION

Graphene oxide and silver nanoparticle nanocomposites were successfully synthesized using a redox chemical reaction. The method involved the electrochemical exfoliation of graphite and the reduction of silver ions by catechol hydroxyl groups during the ultrasonic exfoliation of GO. UV-Vis and FTIR spectra confirmed the presence of C=C and oxygen functional groups in GO. UV-Vis spectra of GO-Ag revealed the presence of GO and nanometallic silver by the surface plasmon resonance (SPR) band around 360 nm. XRD analysis confirmed the successful synthesis of GO in the GO-Ag nanocomposite, indicated by a diffraction peak at $2\theta = 8.6°$. The XRD spectrum of GO-Ag also confirmed the presence of silver nanoparticles with an average size of approximately 15.5 nm, as indicated by the crystalline diffraction pattern of metallic silver. The Raman spectroscopy results showed that the I_D/I_G ratio remained the same for both GO and GO-Ag, indicating that the disordered structure of GO was preserved in the nanocomposite. Notably, the GO-Ag nanocomposite exhibited antimicrobial activity against both tested bacterial strains, highlighting its potential for applications in antimicrobial coatings and treatments. These findings demonstrate the effectiveness of the synthesis method and the promising properties of the GO-Ag nanocomposite for various biomedical and industrial applications.

ACKNOWLEDGEMENTS

The author gratefully acknowledges the financial support from FAPEMIG, CNPq e CAPES.

CREDIT AUTHOR STATEMENT

Rosana Ribeiro Rodrigues: Investigation, Data curation, Formal analysis, Writing-Original draft preparation and editing. **Igor Luiz dos Santos**: Investigation, Data curation, Formal analysis, Writing-Original draft preparation and editing. **Maria Elena Leyva González**: Supervision, Investigation, Conceptualization, Methodology, Writing-Reviewing and Editing. **Adhimar Flávio Oliveira**: Investigation, Data curation, Formal analysis, Writing-Original draft preparation and editing. **Fabio Nakagomi**: Investigation, Data curation, Formal analysis, Writing-Original draft preparation and editing. **Estácio Tavares Wanderley Neto**: Investigation, Data

curation, Formal analysis, Writing-Original draft preparation and editing. **Paulo Sergio Marques**: Investigation, Data curation, Formal analysis, Writing-Original draft preparation and editing. **Eder de Couto Andrade**: Data curation, Formal analysis.

DECLARATIONS

Conflict of interest The authors declare that they have no known competing financial interests or personal relationships that could have appeared to influence the work reported in this paper.

REFERENCES

[1] Burdus, A-C; Gherasim, O.; Grumezescu, A.M.; Mogoantă, L.; Ficai, A.; Andronescu, E. Biomedical Applications of Silver Nanoparticles: An Up-to-Date Overview. Nanomaterials 2018; 8: 681-705. https://doi.org/10.3390/nano8090681.

[2] Bruna, T.; Maldonado-Bravo, F.; Jara, P. Caro, N. Silver Nanoparticles and Their Antibacterial Applications. Int. J. Mol. Sci. 2021; 22: 7202 - 7223. https://doi.org/10.3390/ijms22137202.

[3] Montes-Hernandez, G.; Girolamo, M. D.; Sarret, G.; Bureau,S., Fernandez-Martinez, A.; Lelong,C. and Vernain, E.E. In Situ Formation of Silver Nanoparticles (Ag-NPs) onto Textile Fibers. ACSOmega 2021; 6: 1316−1327. https://dx.doi.org/10.1021/acsomega.0c04814.

[4] Chen C, Li W, Liu X, Yu J, Xing S, Yang J, Han O. Silver nanoparticles/graphene oxide arranged on polytetrafluoroethylene substrate hydrophilic modified with TiO to construct efficient air purification material. J. Environ. Chem. Eng. 2023; 11: 110848. https://doi.org/10.1016/j.jece.2023.110848.

[5] Mikhailova E O. Silver Nanoparticles: Mechanism of Action and Probable Bio-Application. J. Funct. Biomater. 2020: 11: 84. https://doi.org/10.3390/jfb11040084.

[6] Meher A , Tandi A, Moharana S, Chakroborty S , Mohapatra S S, Mondal A, Dey S, Chandra P. Silver nanoparticle for biomedical applications: A review. Hybrid Adv. 2024; 6: 100184. https://doi.org/10.1016/j.hybadv.2024.100184.

[7] Mbayachi V B, Ndayiragije E, Sammani T, Taj S, Mbuta E R, Ullah K. A. Graphene synthesis, characterization and its applications: Results Chem. 2021; 3: 100163. https://doi.org/10.1016/j.rechem.2021.100163.

[8] Dideikin A T and Vul A Y. Graphene Oxide and Derivatives: The Place in Graphene Family. Front. Phys. 2019; 6: 1-13. https://doi.org/10.3389/fphy.2018.00149.

[9] Sadegh K., Zahra A., Ghazaleh E., Arezoo K., Elham B. & Ali Z. An Improved Method for Fabrication of Ag-Go Nanocomposite with Controlled Anti-Cancer and Anti-bacterial Behavior; A Comparative study. Sci. Rep. – Nat. 2019, 9: 9167. https://doi.org/10.1038/s41598-019-45332-7.

[10] Xiaomei C., Genghuang W., Jinmei C., Xi C., Zhaoxiong X., and Xiaoru W. Synthesis of "Clean" and Well-Dispersive Pd Nanoparticles with Excellent Electrocatalytic Property on Graphene Oxide. J. Am. Chem. Soc. 2011; 133: 3693–3695. https://doi.org/10.1021/ja110313d.

[11] Isabella A., Jésus R., Alberto B. and Cécilia M-M. Controlled derivatization of hydroxyl groups of graphene oxide in mild conditions. 2D Mater. 2018; 5: 035037. https://doi.org/10.1088/2053-1583/aac8a9.

[12] Jasmine A. J., Harbir S. M., Nandita B., Tulsi M., and Sudhir K. Role of Phenol Derivatives in the Formation of Silver Nanoparticles. Langmuir 2008; 24: 528-533. https://doi.org/10.1021/la702073r.

[13] Emirua T F, Ayele D W. Controlled synthesis, characterization and reduction of graphene oxide: A convenient method for large scale production. Egypt. J. Basic Appl. Sci. 2017; 4: 74–79. http://dx.doi.org/10.1016/j.ejbas.2016.11.002.

[14] Amendola V. Surface plasmon resonance of silver and gold nanoparticles in the proximity of graphene studied using the discrete dipole approximation method. Phys. Chem. Chem. Phys., 2016; 18: 2230-2241. https://doi.org/10.1039/c5cp06121k.

[15] Tseng K-H, Stobinski L, et al. Interactive Relationship between Silver Ions and Silver Nanoparticles with PVA Prepared by the Submerged Arc Discharge Method. Adv. Mater. Sci. Eng. 2018; 3240959. https://doi.org/10.1155/2018/3240959.

[16] Faniyi I O, Olofinjana B, et al. The comparative analyses of reduced graphene oxide (RGO) prepared via green, mild and chemical approaches. SN Appl. Sci. 2019; 1:1181. https://doi.org/10.1007/s42452-019-1188-7.

[17] Kaja S-S, Aneta K. Joanna G., Karolina B. and Ireneusz P. Elucidation of the function of oxygen moieties on graphene oxide and reduced graphene oxide in the nucleation and growth of silver nanoparticles. RSC Adv. 2016;6: 60056. https://doi.org/10.1039/c6ra10483e.

[18] Drewniak S, Muzyka R, et al. Studies of Reduced Graphene Oxide and Graphite Oxide in the Aspect of Their Possible Application in Gas Sensors. Sensors 2016; 16: 103. https://doi.org/10.3390/s16010103.

[19] Mahmoudia E, Anga W L, et al. Distinguishing characteristics and usability of graphene oxide based on different sources of graphite feed stock. J. Colloid Interface Sci. 2019; 54: 429–440. https://doi.org/10.1016/j.jcis.2019.02.023.

[20] Seabra A B, Manosalva N, et al. Antibacterial activity of nitric oxide releasing silver nanoparticles. IOP Conf. Series: J. Phys: Conf. Ser. 2017; 838:012031. https://doi.org/10.1088/1742-6596/838/1/012031.

[21] Almatroudi A. Silver nanoparticles: synthesis, characterization and biomedical applications. Open Life Sci. 2020; 15: 819–839. https://doi.org/10.1515/biol-2020-0094.

[22] Claramunt S, Varea A, et al. The Importance of Interbands on the Interpretation of the Raman Spectrum of Graphene Oxide. J. Phys. Chem. C. 2015; 119: 10123−10129. https://doi.org/10.1021/acs.jpcc.5b01590.

[23] Anuraga K, Kumara S R. Synthesis of graphene through electrochemical exfoliation technique in aqueous medium. Mater. Today Proc. 2021; 44: 2695–2699. https://doi.org/10.1016/j.matpr.2020.12.684.

[24] Ahmad M A, Aslam S. Synergistic antibacterial activity of surfactant free Ag–GO nanocomposites. Nature Research Sci. Rep. 2021; 11:196. https://doi.org/10.1038/s41598-020-80013-w.

[25] Sandra G. G. S., Silvia E. R., Carolina A-P, Humberto P., Marisa R. V., Anti-adhesion and antibacterial activity of silver nanoparticles and graphene oxide-silver nanoparticle composites. Matéria (Rio J.) 2020; 25:1-9. https://doi.org/10.1590/S1517-707620200002.1071.

[26] Yun'an Q., Lin C., Ruiyan L., Guancong L.,Yanbo Z., Xiongfeng T., Jincheng W., He L., Yanguo Q. Potential antibacterial mechanism of silver nanoparticles and the optimization of orthopedic implants by advanced modification technologies. Int. J. Nanomed. 2018; 13: 3311–3327. https://doi.org/10.2147/IJN.S165125.